CHEMBIOCHEM

DOI: 10.1002/cbic.201200006

A Flavoprotein Monooxygenase that Catalyses a Baeyer–Villiger Reaction and Thioether Oxidation Using NADH as the Nicotinamide Cofactor

Chantel N. Jensen,[a] Jared Cartwright,[b] Jonathan Ward,[a] Sam Hart,[a] Johan P. Turkenburg,[a] Sohail T. Ali,[c] Michael J. Allen,[c] and Gideon Grogan*[a]

A gene from the marine bacterium *Stenotrophomonas maltophilia* encodes a 38.6 kDa FAD-containing flavoprotein (Uniprot B2FLR2) named *S. maltophilia* flavin-containing monooxygenase (SMFMO), which catalyses the oxidation of thioethers and also the regioselective Baeyer–Villiger oxidation of the model substrate bicyclo[3.2.0]hept-2-en-6-one. The enzyme was unusual in its ability to employ either NADH or NADPH as nicotinamide cofactor. The K_M and k_{cat} values for NADH were $23.7 \pm 9.1\ \mu M$ and $0.029\ s^{-1}$ and $27.3 \pm 5.3\ \mu M$ and $0.022\ s^{-1}$ for NADPH. However, k_{cat}/K_M value for the ketone substrate in the presence of 100 μM cofactor was 17 times greater for NADH than for NADPH. SMFMO catalysed the quantitative conversion of 5 mM ketone in the presence of substoichiometric concentrations of NADH with the formate dehydrogenase cofactor recycling system, to give the 2-oxa and 3-oxa lactone products of Baeyer–Villiger reaction in a ratio of 5:1, albeit with poor enantioselectivity. The conversion with NADPH was 15%. SMFMO also catalysed the NADH-dependent transformation of prochiral aromatic thioethers, giving in the best case, 80% *ee* for the transformation of *p*-chlorophenyl methyl sulfide to its *R* enantiomer. The structure of SMFMO reveals that the relaxation in cofactor specificity appears to be accomplished by the substitution of an arginine residue, responsible for recognition of the 2′-phosphate on the NADPH ribose in related NADPH-dependent FMOs, with a glutamine residue in SMFMO. SMFMO is thus representative of a separate class of single-component, flavoprotein monooxygenases that catalyse NADH-dependent oxidations from which possible sequences and strategies for developing NADH-dependent biocatalysts for asymmetric oxygenation reactions might be identified.

Introduction

Flavoprotein monooxygenases (FPMOs) catalyse many reactions of potential interest for application in catalytic asymmetric synthesis. A review by van Berkel and Fraaije in 2006 has grouped these enzymes into six classes, A–F.[1] Of these, the Baeyer–Villiger monooxygenases (BVMOs) and flavin-containing monooxygenases (FMOs), each from class B, have proved to be particularly interesting in respect of their ability to catalyse enantioselective oxidation reactions (Scheme 1). BVMOs[2] catalyse the insertion of oxygen adjacent to a carbonyl group, an important transformation in synthetic organic chemistry for the peracid-mediated conversion of ketones to esters or lactones. They utilise a nicotinamide cofactor (commonly NADPH) to reduce a flavin coenzyme FAD to $FADH_2$, which then reacts with molecular oxygen to form a flavin hydroperoxidate, which is thought to be the active catalyst in the oxygen-insertion reaction.[3] The most common class B BVMOs, typified by the cyclohexanone monooxygenase (CHMO) from *Acinetobacter*,[4] are single polypeptides of approximately 55–65 kDa and have the ability to catalyse both NADPH-dependent reduction of FAD and also the substrate oxygenation reaction within their active site. BVMOs have also been shown to catalyse the asymmetric electrophilic oxidation of prochiral thioethers to produce chiral sulfoxide products with high enantioselectivity.[5]

Class B FMOs also typically consist of a single polypeptide that has the ability to both reduce flavin and oxidise their substrates using, in this case, a flavin hydroperoxide.[1] They again use NADPH to reduce FAD, and use the flavin hydroperoxide to oxidise heteroatoms such as sulfur and nitrogen.[6] FMOs do not usually catalyse Baeyer–Villiger oxidations, perhaps because they lack a conserved arginine residue thought to be necessary for stabilisation of the peroxidate anion required for oxygen insertion reactions.[1] There are some reports of FMO-catalysed Baeyer–Villiger reactions however,[7] although the basis of peroxidate stabilisation in those processes is not yet fully understood. The profile of FMOs is increasing with respect to their application as biocatalysts, particularly in the oxidation of thioethers to optically active sulfoxides.[8]

In the cases of both BVMOs and FMOs, one of the drawbacks from the perspective of industrial application is the dependence of the enzymes on the phosphorylated nicotinamide

[a] C. N. Jensen, J. Ward, S. Hart, Dr. J. P. Turkenburg, Dr. G. Grogan
Department of Chemistry, University of York
Heslington, York, YO10 5DD (UK)
E-mail: gideon.grogan@york.ac.uk

[b] Dr. J. Cartwright
Technology Facility, Department of Biology, University of York,
YO10 5DD York (UK)

[c] S. T. Ali, Dr. M. J. Allen
Plymouth Marine Laboratory
Prospect Place, Plymouth PL1 3DH (UK)

Supporting information for this article is available on the WWW under http://dx.doi.org/10.1002/cbic.201200006.

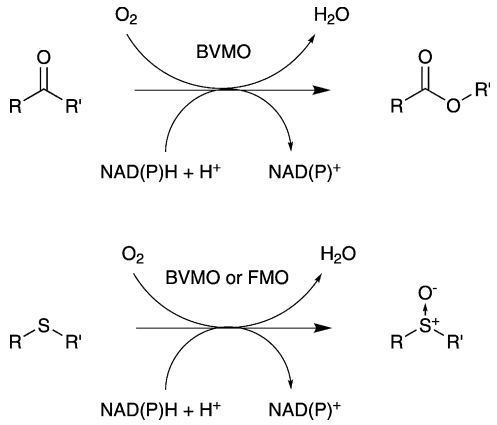

Scheme 1. Baeyer–Villiger oxidation and sulfoxidation reactions catalysed by flavin-dependent Baeyer–Villiger monooxygenases (BVMOs) and flavin monooxygenases (FMOs). NAD(P)H is used to reduce the flavin prior to reaction with molecular oxygen, yielding a flavin hydroperoxidate, or hydroperoxide, which is the oxidant in the reaction(s).

cofactor NADPH. NADPH is more expensive than its nonphosphorylated analogue NADH, and hence attempts have been made to investigate or engineer the cofactor preference of BVMOs, based on structural analysis of the active site interactions with the phosphate of NADPH.[9,10] However, success in this regard has been limited, suggesting that the simple engineering of NADH specificity in NADPH-dependent enzymes is not a trivial undertaking. NADH-dependent BVMO activity has been reported,[11,12] but in those enzymes (class C FPMOs[1]) the flavin reduction and substrate oxygenation domains are separate polypeptides, and the transfer of reduced flavin ($FMNH_2$ in those cases) between proteins for catalysis presents additional complications with respect to application.

In this report, we describe the cloning and expression of a gene encoding a single-component flavoprotein monooxygenase, *S. maltophilia* flavin-containing monooxygenase (SMFMO), capable of Baeyer–Villiger oxidation and sulfoxidation reactions, which is able to use NADH as well as NADPH as a nicotinamide cofactor. The structure of SMFMO also reveals the molecular determinants of cofactor promiscuity when compared to NADPH-dependent FMOs. Characterisation of the purified recombinant enzyme is reported, along with its application to the oxidation of a series of commonly used substrates for BVMOs and FMOs. Whilst the enantioselectivity of the enzyme is only low to moderate, the study points to a new subfamily of flavoprotein targets that might be exploited or evolved for improved asymmetric oxidations with considerable economic advantages over NADPH-dependent enzymes.

Results and Discussion

Identification of SMFMO gene

As part of studies directed towards characterising new FMO and BVMO activity,[13] analysis of the genome sequence of the marine isolate *Stenotrophomonas maltophilia*[14] revealed a putative open-reading frame, encoding an enzyme (SMFMO, Uniprot Code B2FLR2) with an amino acid motif typical of an FMO (**FAG**IQL**H**SAH**Y**)[1]), and two Rossman motifs (GXGXXG) for the binding of ADP moiety of the FAD and NADPH, as typically observed in class B FMOs (see Figure S1 in the Supporting Information). The putative molecular weight of the encoded protein was 38 558 kDa, significantly smaller than class B bacterial FMOs that have been fully characterised such as mFMO from *Methylophaga aminisulfidovorans* (2XLT, 2XVI, 53.0 kDa[15,16]). A BLAST search of the Swissprot database using the SMFMO translated gene sequence revealed closest sequence homology to shorter "putative flavin monooxygenases" from strains such as *Pseudomonas*, but also pyridine nucleotide disulfide oxidoreductase family enzymes including thioredoxin reductases (TrxRs).

The sequence homology with TrxRs is instructive, as a sequence-based search of the RCSB Protein Structure database also revealed that the closest sequence homology to proteins for which the structure had been solved also includes TrxRs, such as those from *Thermus thermophilus* (2ZBW) and *Helicobacter pylori* (2Q0K), as well as BVMOs [PAMO (1W4X) and CHMO from *Rhodococcus* (3GWD)] and FMOs from *S. pombe* (2V8) and *Methylophaga* spp (2XVI, 2XLT). A phylogenetic tree (Figure 1) featuring representative sequences of BVMOs, FMOs and TrxRs shows that SMFMO features on a branch as closely related to TrxRs, with which it has most similarity in overall length and sequence similarity, as to BVMOs or FMOs. A sequence alignment of some representative enzymes from Figure 1 is shown in Figure S2.

Cloning, expression and purification

A version of the gene encoding SMFMO was synthesised using a sequence optimised for codon usage in *E. coli*, amplified using PCR and cloned into an expression vector for production of the enzyme in *E. coli*. The enzyme was then purified using nickel-affinity chromatography and gel filtration (Figure S3) to yield an enzyme of bright yellow colour. Calibrated size-exclusion chromatography suggested the enzyme to be a dimer in solution and the presence of FAD was confirmed by LCMS analysis of boiled enzyme extracts against boiled, standard samples of FAD and FMN using an established procedure.[17]

Enzyme assays

In preliminary experiments, pure SMFMO was assayed for class B FPMO-type activity using GC analysis of biotransformations of the standard FMO substrate *p*-tolyl methyl sulfide (**1**, Scheme 2) in the presence of either NADPH or NADH as nicotinamide cofactor. Interestingly, SMFMO was capable of oxidation of a thioether substrate using either cofactor. SMFMO was then assayed for its ability to catalyse Baeyer–Villiger oxidation of the standard BVMO substrate bicyclo[3.2.0]hept-2-en-6-one (**3**). Again, activity was observed using either reduced nictotinamide cofactor, despite the enzyme being structurally dissimilar to known NADPH-dependent BVMOs, which are typically enzymes of approximately 60 kDa molecular weight. Kinetic studies of cofactor utilisation by SMFMO were performed

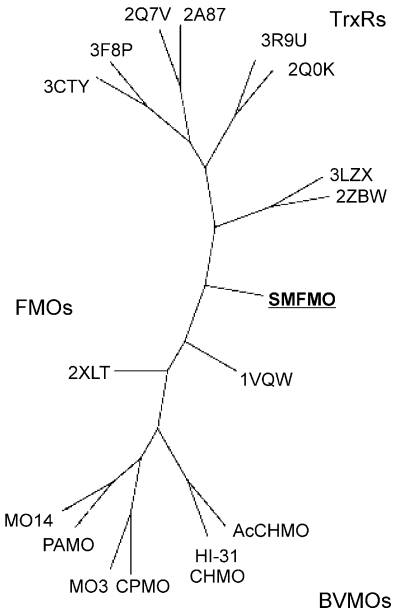

Figure 1. Phylogenetic tree showing position of *Stenotrophomonas maltophila* flavin-containing monooxygenase **SMFMO** in the context of some BVMOs, FMOs, and related flavin-binding thioredoxin reductases (TrxRs) for which structure and/or function has been described. **BVMOs**: HI-31 CHMO = Cyclohexanone monooxygenase from *Rhodococcus* sp. HI-31 (3GWD, Uniprot C0STX7); AcCHMO = Cyclohexanone monooxygenase from *Acinetobacter calcoaceticus* (Uniprot Q9R2F5); MO14 = ro03437 from *Rhodococcus jostii* RHA1 (Uniprot Q0SB46); MO3 = ro03247 from *Rhodococcus jostii* RHA1 (Uniprot Q0SBN6); PAMO = phenylacetone monooxygenase from *Thermobifida fusca* (Uniprot Q47PU3); CPMO = Cyclopentanone monooxygenase from *Comamonas* sp. (Uniprot Q8GAW0); **TrxRs**: 3F8P = TrxR from *Sulfolobus solfataricus* (Uniprot Q8X236); 3CTY = TrxR from *Thermoplasma acidophilum* (Uniprot Q9HJI4); 2A87 = TrxR from *Mycobacterium tuberculosis* (Uniprot P52214); 2Q7V = thioredoxin reductase from *Deinococcus radiodurans* (Uniprot Q9RSY7); 2Q0K = thioredoxin reductase from *Helicobacter pylori* (Uniprot P56431); 3R9U = TrxR from *Campylobacter jejuni* (Uniprot Q0PBZ1); 3LZX = ferredoxin-NADP$^+$ oxidoreductase from *Bacillus subtilis* (Uniprot O05268); 2ZBW = TrxR-like protein from *Thermus thermophilus* (Uniprot Q5L28); **FMOs**: 1VQW = Flavin-containing monooxygenase from *Schizosaccharomyces pombe* (Uniprot Q9HFE4); 2XVI = FMO from *Methylophaga aminisulfidivirans* (Uniprot Q83K4).

Table 1. Kinetic constants for SMFMO using NADH or NADPH as cofactor, with substrate **3**.

Experiment	K_M [μmol dm^{-3}]	V_{max} [μmol dm^{-3} s^{-1}]	k_{cat} [s^{-1}]	k_{cat}/K_M [μmol dm^{-3} s^{-1}]
NADH + 100 μM **3**	23.7 ± 9.1	11.2 ± 1.5 × 10^{-2}	0.029	1223
NADPH + 100 μM **3**	27.3 ± 5.3	8.4 ± 0.6 × 10^{-2}	0.022	806
3 + 100 μM NADH	0.07 ± 0.03	1.4 ± 0.2 × 10^{-2}	3.6 × 10^{-3}	51
3 + 100 μM NADPH	3.20 ± 0.90	3.3 ± 0.3 × 10^{-2}	8.5 × 10^{-3}	3

using the method described for hydroxyacetophenone monooxygenase (HAPMO),[10] using either cofactor in the presence of 100 μM of the ketone substrate **3** (Table 1, Figure S4).

The apparent K_M and V_{max} values for NADH and NADPH in this assay were comparable, in the region of 20–30 μM, indicative of an equal capability for the use of either cofactor to reduce flavin in the enzyme, and are comparable with the NADPH oxidase activity of, for example mFMO from *Methylophaga* (13 μM and 0.06 s^{-1}).[15] Kinetic constants for substrate **3** were then determined in the presence of 100 μM of either cofactor (Table 1, Figure S5 A and B in the Supporting Information). In these cases, Michaelis–Menten behaviour with respect to **3** was observed, with the K_M value for the ketone substrate in the presence of NADH approximately 42 times lower, and k_{cat}/K_M value 17 times higher than for NADPH. The V_{max} value for the ketone with NADH (1.4 × 10^{-2} μM s^{-1}) is appreciably smaller than that usually observed for BVMOs acting on ketones, but is within the range of, for example the FPMO MtmOIV, when expressed in the same terms (5 nmol min mg^{-1} protein versus 147 nmol min mg^{-1} [18]), and in that case MtmOIV was acting on its natural substrate.

Substrate selectivity and enantioselectivity

A range of class B FPMO ketone substrates was then tested as substrates for SMFMO, using either NADH or NADPH as nicoti-

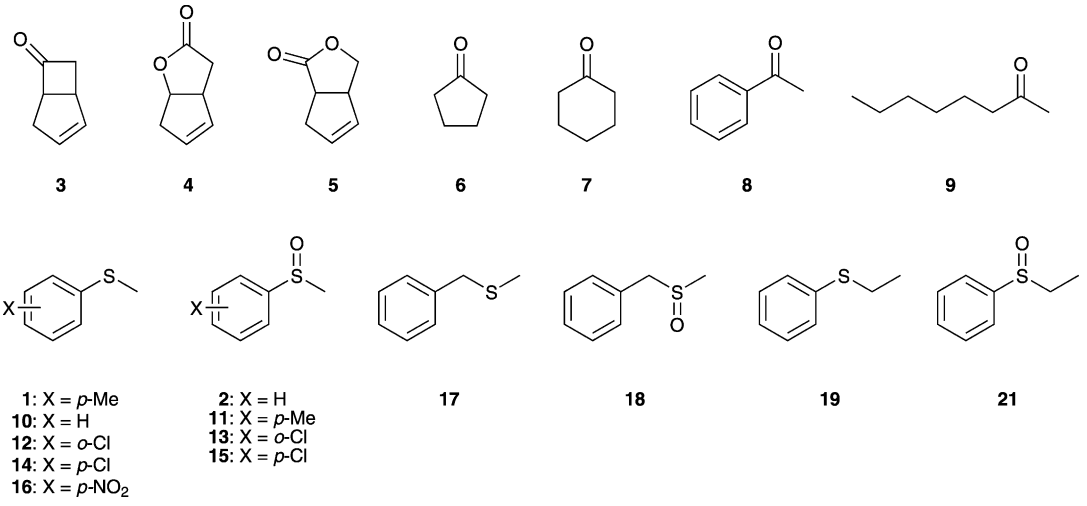

Scheme 2. Test substrates and products used in this study.

namide cofactor, and the appropriate cofactor recycling systems: formate dehydrogenase and sodium formate for NADH and glucose-6-phosphate dehydrogenase and glucose-6-phosphate for NADPH. The Baeyer–Villiger oxidation activity of SMFMO was restricted to the strained, fused cyclobutanone system of substrate **3**, with many simpler aliphatic and alicylic ketones (Scheme 2) such as cyclopentanone (**6**), cyclohexanone (**7**), acetophenone (**8**) and octan-2-one (**9**) not transformed with either cofactor. Conversion of **3** was appreciably higher when NADH was employed as cofactor with 93% conversion observed compared to 15% with NADPH over a 24 h period. The NADH-dependent transformation of **3** was found to be regioselective in the manner of peracid-mediated Baeyer–Villiger oxidations of this substrate, giving a yield of regioisomers in the ratio 5:1 in favour of the "normal" 2-oxa lactone over the "abnormal" 3-oxa product. Enantioselectivity was poor, but measurable, with 8% *ee* for (1*R*,5*S*)-(+)-**4** and 36% *ee* for (1*S*, 5*R*)-**5**. Chiral GC analysis of the residual ketone showed it to be racemic.

More promiscuous substrate selectivity was observed in the transformation of prochiral thioether substrates by SMFMO (Table 2). Conversions were observed for phenyl methyl sulfide (**10**), *p*-tolyl methyl sulfide (**1**), *o*- and *p*-chlorophenyl methyl sulfide (**12** and **14** respectively), benzyl methyl sulfide **(17**) and phenyl ethyl sulfide (**19**). *p*-Nitrophenyl methyl sulfide (**16**) was not transformed. In each case, greater conversions were achieved using NADH as cofactor, and enantiomeric excess of products was dependent on the substrate structure. The preferred enantiomeric series in sulfoxidation by SMFMO [(*R*)-] was in most cases the same as that encountered for chloroperoxidase.[19] In most cases, and most notably for **10**, the enantioselectivity was poorer than for CHMO[5,20] or mFMO,[8] but it was superior in the case of substrate **14** and in the opposite enantiomeric series.

Table 2. Results of biotransformations of prochiral thioether substrates by SMFMO.

Thioether substrate	Conversion [%]		*ee* [%]	
	using NADH	using NADPH	using NADH	using NADPH
1	90	33	25 (*R*)	44 (*R*)
10	8	1	21 (*R*)	n.d.
12	6	0.2	15 (*S*)	n.d
14	40	9	80 (*R*)	82 (*R*)
16	0	0	–	–
17	32	10	24 (*R*)	38 (*R*)
19	27	2	71 (*R*)	57 (*R*)

n.d.: not determined.

Structure of SMFMO

In order to investigate the molecular determinants of cofactor promiscuity in SMFMO, the X-ray structure of SMFMO was solved and refined to a resolution of 2.72 Å. SMFMO exists as a dimer (Figure 2) and its monomeric tertiary structure is most similar to the structure of putative FMO 3D1C in the Protein Databank, with which it shares only 16% sequence identity. It also shares some structural motifs with known FMOs such as mFMO (2XLT, 2XIV),[15,16] to BVMOs such as 3GWD from *Rhodococcus*[23] and also to enzymes of the thioredoxin family of proteins such as that from *Thermus thermophilus* (2ZBW).

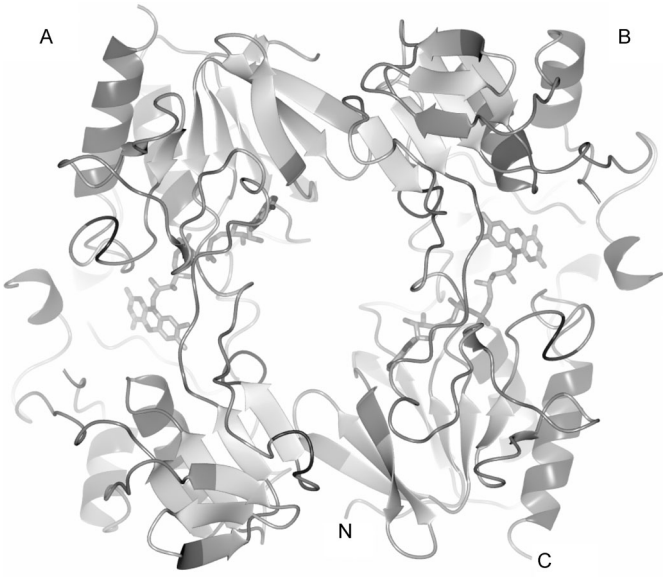

Figure 2. Quaternary structure of dimeric SMFMO showing the two subunits A and B. Protein backbone is shown in ribbon format. FAD molecules (one per subunit) are shown in cylinder format. The N and C termini of subunit B are also indicated.

Each monomer of SMFMO is complexed with FAD, and is complete apart from a loop of approximately twenty amino acids between positions 212 and 233, which may constitute a flexible loop that covers the active site containing the flavin, and could not be modelled. Although the structure is not in complex with NAD(P)H, the putative binding sites of the nicotinamide cofactor phosphates, including that which is on the 2′-hydroxyl of ribose, and distinguishes NADP(H) from NAD(H), are occupied with sulfate, which was used in 0.9 M concentration in the crystallisation drop. Superimposition of NADPH-dependent FMO structure 2XLT, which is complexed with both FAD and NADPH, with SMFMO clearly reveals that the Arg234 (and Thr235) residue of NADPH-dependent enzymes of this type, which is involved in binding the ribose phosphate, is replaced by a glutamine residue Gln193 (and His 194) in SMFMO (Figure 3). Specificity for NADPH appears therefore to have been relaxed owing to the removal of interactions between the positively charged arginine side chain and the negatively charged phosphate oxygen(s).

It has been reported[24] that $NADP^+$ fulfils dual roles in FPMOs: helping to stabilise the flavin oxygenating species after flavin reduction and reaction with oxygen. The superior activity of SMFMO towards substrates on addition of NADH rather than NADPH suggests that this stabilisation may be better supplied by the nonphosphorylated cofactor. However, the molecular basis of stabilisation of a flavin hydroperoxide for sulfoxidation by SMFMO is still unresolved. In mFMO, Asn78 is thought to provide this stabilisation, and activity is removed even by mutation to serine.[24] SMFMO features the

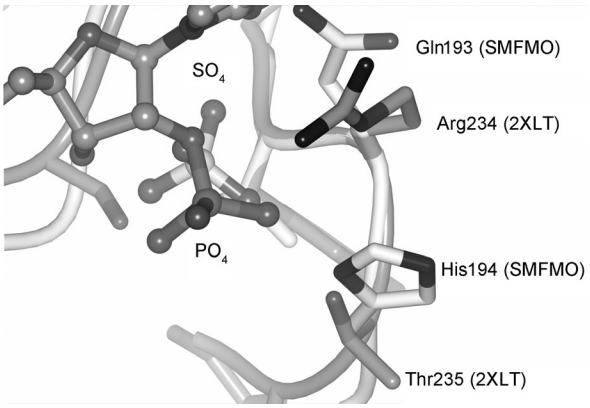

Figure 3. NADP ribose 2′-phosphate recognition site in mFMO (2XLT: backbone, side chains and NADP carbon atoms in grey), superimposed with structurally homologous region of SMFMO (white) bound to sulfate, illustrating replacement of Arg234 and Thr235 in NADPH-dependent 2XLT with Gln193 and His 194 in SMFMO of relaxed cofactor specificity.

large, hydrophobic Phe52 in this position (Figure S6). However, it has recently been shown that hydrophobic residues in this region are tolerated by flavin-dependent oxidases and oxygenases, and that oxygen activation depends very much on the active site context.[25]

The ability of SMFMO to catalyse BV reactions is more difficult to explain. The hydroperoxidate held to be the oxidising species in enzymatic Baeyer–Villiger reactions is thought to be stabilised by an arginine residue, Arg337 in PAMO, which is conserved in all known BVMOs, yet absent in SMFMO. The determinants of Baeyer–Villiger activity in SMFMO are currently under investigation using mutation experiments.

Conclusion

The characterisation of SMFMO has identified a type of single-component FPMO capable of NADH-dependent oxygenation reactions, and determined the structural basis for relaxed nicotinamide cofactor promiscuity in this enzyme. This will help to highlight other, related enzymes in the database, providing a possible platform for developing NADH-dependent FPMOs for asymmetric oxygenation reactions.

Experimental Section

Gene cloning and expression: The gene encoding SMFMO (B2FLR2) was obtained using commercial DNA synthesis of a codon-optimised sequence prepared in the plasmid pBlue-ScriptSK from Geneart (Regensburg, Germany). The gene was then amplified by PCR using the following primers: CCAGG GACCA GCAAT GGATA GTGTA GACGT TGTAG TTATT GGTG (forward)/ GAGGA GAAGG CGCGT TAACG GTCCT GGTGA TCGGC GCAG (reverse) for cloning into the pET-YSBL-LIC-3C vector using an established ligation-independent cloning (LIC) procedure.[26] The resulting construct yielded an N-terminal fusion of a hexahistidine tag with a 3C-protease cleavage site (pET-YSBL-LIC-3C) under the control of the T7 promoter. The recombinant plasmid was used to transform *E. coli* XL1-Blue cells (Novagen) and plasmids recovered from the recombinant strains by standard miniprep procedures were submitted for sequencing to confirm the integrity of the gene.

Enzyme purification: The pET-YSBLIC-3C vector containing the SMFMO gene was used to transform cells of *E. coli* BL21 (DE3) using kanamycin (30 $\mu g\,mL^{-1}$) as antibiotic marker on Luria Bertani (LB) agar. A single colony of a plate grown overnight was used to inoculate 4×5 mL of LB broth, which were grown overnight at 37 °C with shaking at 180 rpm. The starter cultures were then used to inoculate LB broth (4×500 mL cultures) in which cells were grown until the optical density (OD_{600}) of the culture had reached approximately 0.6. At this point the expression of SMFMO was induced by the addition of isopropyl β-D-1-thiogalactopyranoside (IPTG, final concentration of 1 mM). The cultures were then incubated at 18 °C in an orbital shaker overnight at 180 rpm. After approximately 18 h growth, the cells in each case were harvested by centrifugation (4225 *g*, 15 min) in a Sorvall RC5B Plus centrifuge and were then resuspended collectively in Tris·HCl buffer (100 mL, 50 mM, pH 7.5, henceforth referred to as "buffer") containing sodium chloride (300 mM). Cells were disrupted by ultrasonication for 3×30 s bursts at 4 °C with 1 min intervals and the soluble and insoluble material fractions separated by centrifugation (26892 *g*, 30 min). The supernatant, containing the soluble SMFMO, was loaded onto a 5 mL His-Trap Chelating HP nickel column. After washing with buffer (10 column volumes containing 30 mM imidazole) enzyme was eluted using an imidazole gradient (30–500 mM imidazole over 20 column volumes of eluant). Column fractions were analysed by SDS PAGE and those bright yellow fractions containing a pure 38 kDa protein were pooled and concentrated using a 10 kDa cut-off Centricon filter membrane. Concentrated protein was loaded onto an S75 Superdex gel filtration column that had been equilibrated with buffer, and eluted with buffer (120 mL). Fractions containing pure protein were pooled and stored at −20 °C.

Enzyme assays: Steady-state kinetic constants for NADH and NADPH in the presence of ketone substrate **3** (see main text) were determined using the method employed for HAPMO by Kamerbeek et al.[10] In a 1 mL quartz cuvette containing Tris·HCl buffer (pH 7.5, 50 μmol) and ketone **3** (100 nmol), the decrease in absorbance at 340 nm was monitored at concentrations of NAD(P)H (10–100 μM) after the addition of enzyme (3.9 nmol). The results are shown in Figure S5. Kinetic constants were calculated using a value for ε of 6220 $mol\,dm^{-3}\,cm^{-1}$. Kinetic constants for substrate **3** were determined using the method employed for MtmOIV by Röhr and co-workers.[18] The oxidation of NADPH or NADH (100 μM) was monitored in the presence of a range of concentrations of substrate **3** (0–20 mM) after the addition of SMFMO (3.9 nmol). The results are shown in Figure S5 A and B. All data points represent the average of two separate runs.

Biotransformations: Biotransformations using isolated enzyme with cofactor recycling were performed using the method of Faber and co-workers.[27] For NADH-dependent biotransformations: To a 10 mL round bottomed flask containing Tris·HCl buffer (pH 7.5, 5 mL) were added substrate(s) (**1, 3, 6**–**9**, **10**, **12**, **14**, **16**, **17** or **19** in ethanol (100 μL) to a final concentration of 5 mM), NADH (5 mg, a final concentration of 0.7 mM), formate dehydrogenase (5 mg), sodium formate (6.8 mg, 0.1 mmol) and SMFMO (1 mL of a 5 $mg\,mL^{-1}$ solution, 0.13 μmol). The reactions were then stirred for 24 h at room temperature. Aliquots (500 μL) were taken at intervals and extracted with ethyl acetate (500 μL). The organic layer was transferred to a GC vial and analysed by GC. For NADPH-dependent biotransformations: To a 10 mL round bottomed flask containing Tris·HCl buffer (pH 7.5, 5 mL) were added substrate(s)

(**1, 3, 6**–**9**, **10**, **12**, **14**, **16**, **17** or **19** in ethanol (100 μL) to a final concentration of 5 mM), NADPH (5.7 mg, a final concentration of 0.7 mM), glucose-6-phosphate-dehydrogenase (0.14 mg), glucose-6-phosphate (5.2 mg, 0.02 mmol) and SMFMO (1 mL of a 5 mg mL^{-1} solution, 0.13 μmol). The reactions were then stirred for 24 h at room temperature and organic extracts of 500 μL aliquots analysed as described above.

GC analysis: For all standard GC analysis, an Agilent HP-6890 gas chromatograph fitted with a HP-5 column (30 m × 0.32 mm × 0.25 μm) was used. The injector temperature was set at 250 °C and the detector temperature was 320 °C. Helium was used as the carrier gas at a pressure of 83 kPa. Details of programmes used for analysis of substrates **1, 3**–**9**, **10**, **12**, **14**, **16**, **17** or **19** can be found in Table S1. Chiral GC analysis of substrate **3** was performed using the same GC apparatus equipped with a BGB-175 column (30 m × 0.25 mm × 0.25 μm, BGB-Analytik) using a temperature gradient of 100 °C to 127 °C at 2 °C min^{-1}. Chiral analysis of products **2** and **3** was performed using a BGB-173 column (30 m × 0.25 mm × 0.25 μm, BGB Analytik) with a temperature gradient of 90–34 °C at 1 °C min^{-1}. The enantiomeric excesses of products **2**, **11**, **13**, **15**, **18** and **20** were measured using the BGB-173 column. Racemic sulfoxide standards were prepared from the substrates by oxidation with hydrogen peroxide and acetic acid.[28] Absolute configurations of products were assigned through comparison with products of biotransformations using cyclohexanone monooxygenase, in conjunction with results reported for that enzyme.[5,20]

Crystallisation of SMFMO: Pure SMFMO was subjected to crystallisation trials using a range of commercially available screens in 96-well plates using 300 nL drops at a range of protein concentrations. The best crystals were obtained using the Clear Strategy Screen[29] in conditions containing 1.8 M lithium sulphate (1.8 M) and protein (4 mg mL^{-1}). Larger crystals for diffraction analysis using optimised conditions were prepared using the hanging-drop vapour diffusion method in 24-well plate Linbro dishes and using crystallisation drops of 2 μL with protein (4 mg mL^{-1}). The best crystals were routinely obtained in crystal drops containing lithium sulphate (0.9 M) in Bis-Tris propane buffer (100 mM) at pH 5.6. Crystals were tested for diffraction using a Rigaku Micromax-007HF generator fitted with Osmic multilayer optics and a MARRESEARCH MAR345 imaging plate detector. Those crystals that diffracted to greater than 3 Å resolution were flash-cooled in liquid nitrogen in a cryogenic solution containing the mother liquor containing also 10% *w/v* glycerol and retained for data collection at the synchrotron.

Data collection, structure solution, model building and refinement of SMFMO structure: A complete dataset was collected on beamline id142 at the European Synchrotron Radiation Facility, Grenoble on 3rd March 2010. Data were processed using the HKL2000[30] interface and the data collection statistics are given in Table S2. The crystals were in space group $P3_2$. The structure was solved using the program BALBES,[31] which found a solution using separate domains of the thioredoxin reductase from *Thermoplasma acidophilum* 3CTY[32] as a model. The solution contained two molecules in the asymmetric unit. The structure was improved using iterative rounds of building in Autobuild in the Phenix suite of programmes[33] and refinement using REFMAC.[34] In refinement, non-crystallographic symmetry (NCS) restraints were applied for chain B against chain A. After building the protein and water molecules, FAD was modelled into clear residual density in the difference maps, to yield the structure of the dimeric holoenzyme. The FAD isoalloxazine ring was clearly puckered, indicative of at least a partial population of the reduced state $FADH_2$ (Figure S6). The final structure exhibited R_{cryst} and R_{free} values of 18.6 and 23.9% respectively and was finally validated using PROCHECK.[35] Data collection and refinement statistics are presented in Table S2. The Ramachandran plot showed 92.3% of residues to be situated in the most favoured regions, 7.4% in additional allowed and only Tyr139 residues in each subunit exhibiting unusual backbone conformations. The coordinates and structure factors have been deposited in the Protein Databank with the accession code 4a9w.

Acknowledgements

We are grateful to the Biotechnology and Biological Sciences Research Council and PML Applications Ltd. for funding a CASE studentship to C.N.J., and to Karl Heaton for LC-MS experiments.

Keywords: Baeyer–Villiger monooxygenase · biotransformation · flavoprotein · NADPH · oxidoreductase

[1] W. J. H. van Berkel, N. M. Kamerbeek, M. W. Fraaije, *J. Biotechnol.* **2006**, *124*, 670 – 689.
[2] D. E. Torres Pazmiño, H. M. Dudek, M. W. Fraaije, *Curr. Opin. Chem. Biol.* **2010**, *14*, 138 – 144.
[3] D. Sheng, D. P. Ballou, V. Massey, *Biochemistry* **2001**, *40*, 11156 – 11167.
[4] N. A. Donoghue, D. B. Norris, P. W. Trudgill, *Eur. J. Biochem.* **1976**, *63*, 175 – 192.
[5] S. Colonna, N. Gaggero, P. Pasta, G. Ottolina, *Chem. Commun.* **1996**, 2303 – 2307.
[6] M. A. Hamman, B. D. Haehner-Daniels, S. A. Wrighton, A. E. Rettie, S. D. Hall, *Biochem. Pharmacol.* **2000**, *60*, 7 – 17.
[7] W. G. Lai, N. Farah, G. A. Moniz, Y. N. Wong, *Drug Metab. Dispos.* **2011**, *39*, 61 – 70.
[8] A. Rioz-Martinez, M. Kopacz, G. de Gonzalo, D. E. Torres Pazmiño, V. Gotor, M. W. Fraaije, *Org. Biomol. Chem.* **2011**, *9*, 1337 – 1341.
[9] H. Dudek, D. Torres Pazmiño, C. Rodríguez, G. de Gonzalo, V. Gotor, M. W. Fraaije, *Appl. Microbiol. Biotechnol.* **2010**, *88*, 1135 – 1143.
[10] N. M. Kamerbeek, M. W. Fraaije, D. B. Janssen, *Eur. J. Biochem.* **2004**, *271*, 2107 – 2116.
[11] K. H. Jones, R. T. Smith, P. W. Trudgill, *J. Gen. Microbiol.* **1993**, *139*, 797 – 805.
[12] R. Villa, A. Willetts, *J. Mol. Catal. B* **1997**, *2*, 193 – 197.
[13] C. Szolkowy, L. D. Eltis, N. C. Bruce, G. Grogan, *ChemBioChem* **2009**, *10*, 1208 – 1217.
[14] M. J. Allen, K. Tait, K. Weynberg, C. Bradley, U. Trivedi, M. Blaxter, I. Joint, J. Nissimov, C. N. Jensen, G. Grogan, M. Muhling, S. T. Ali, *manuscript submitted*.
[15] A. Alfieri, E. Malito, R. Orru, M. W. Fraaije, A. Mattevi, *Proc. Natl. Acad. Sci. USA* **2008**, *105*, 6572 – 6577.
[16] H. J. Cho, H. Y. Cho, K. J. Kim, M. H. Kim, S. W. Kim, B. S. Kang, *J. Struct. Biol.* **2011**, *175*, 39 – 48.
[17] Q. Yu, P. Schaub, S. Ghisla, A. Al-Babili, A. Krieger-Liszkay, P. Bayer, *J. Biol. Chem.* **2010**, *285*, 12109 – 12120.
[18] M. Gibson, M. Nur-e-alam, F. Lipata. M. A. Oliveira, J. Rohr, *J. Am. Chem. Soc.* **2005**, *127*, 17594 – 17595.
[19] S. Colonna, N. Gaggero, A. Manfredi, L. Casella, M. Gullotti, G. Carrea, P. Pasta, *Biochemistry* **1990**, *29*, 10465 – 10468.
[20] G. Carrea, B. Redigolo, S. Riva, S. Colonna, N. Gaggero, E. Battistel, D. Bianchi, *Tetrahedron: Asymmetry* **1992**, *3*, 1063 – 1068.
[21] D. E. Torres Pazmiño, R. Snajdrova, D. V. Rial, M. D. Mihovilovic, M. W. Fraaije, *Adv. Synth. Catal.* **2007**, *349*, 1361 – 1368.
[22] M. T. Reetz, F. Daligault, B. Brunner, H. Hinrichs, A. Deege, *Angew. Chem.* **2004**, *116*, 4170 – 4173; *Angew. Chem. Int. Ed.* **2004**, *43*, 4078 – 4081.
[23] I. A. Mirza, B. J. Yachnin, S. Wang, S. Grosse, H. Bergeron, A. Imura, H. Iwaki, Y. Hasegawa, P. C. K. Lau, A. M. Berghuis, *J. Am. Chem. Soc.* **2009**, *131*, 8848 – 8854.
[24] R. Orru, D. E. Torres-Pazmiño, M. W. Fraaije, A. Mattevi, *J. Biol. Chem.* **2010**, *285*, 35021 – 35028.

[25] C. A. McDonald, R. L. Fagan, F. Collard, V. M. Monnier, B. A. Palfey, *J. Am. Chem. Soc.* **2011**, *133*, 16809 – 16811.
[26] K. E. Atkin, R. Reiss, N. J. Turner, A. M. Brzozowski, G. Grogan, *Acta Crystallogr. Sect. F Struct. Biol. Cryst. Commun.* **2008**, *64*, 182 – 185.
[27] M. Hall, C. Stueckler, W. Kroutil, P. Macheroux, K. Faber, *Angew. Chem.* **2007**, *119*, 4008 – 4011; *Angew. Chem. Int. Ed.* **2007**, *46*, 3934 – 3937.
[28] H. Golchoubian, F. Hosseinspoor, *Molecules* **2007**, *12*, 304 – 311.
[29] A. M. Brzozowski, J. Walton, *J. Appl. Crystallogr.* **2001**, *34*, 97 – 101.
[30] Z. Otwinowski, W. Minor, *Methods Enzymol.* **1997**, *276*, 307 – 326.
[31] F. Long, A. A. Vagin, P. Young, G. N. Murshudov, *Acta. Crystallogr. Sect. D. Biol. Crystallogr.* **2008**, *64*, 125 – 132.
[32] H. H. Hernandez, O. A. Jaquez, M. J. Hamill, S. J. Elliott, C. L. Drennan, *Biochemistry* **2008**, *47*, 9728 – 9737.
[33] P. D. Adams, P. V. Afonine, G. Bunkóczi, V. B. Chen, I. W. Davis, N. Echols, J. J. Headd, L.-W. Hung, G. J. Kapral, R. W. Grosse-Kunstleve, A. J. McCoy, N. W. Moriarty, R. Oeffner, R. J. Read, D. C. Richardson, J. S. Richardson, T. C. Terwilliger, P. H. Zwart, *Acta. Crystallogr. Sect. D. Biol. Crystallogr.* **2010**, *66*, 213 – 221.
[34] G. N. Murshudov, A. A. Vagin, E. J. Dodson, *Acta. Crystallogr. Sect. D. Biol. Crystallogr.* **1997**, *53*, 240 – 255.
[35] R. A. Laskowski, M. W. Macarthur, D. S. Moss, J. M. Thornton, *J. Appl. Crystallogr.* **1993**, *26*, 283 – 291.

Received: January 4, 2012
Published online on March 13, 2012

